Plant host identity drives *Andropogon gerardi*i rhizobiome assembly strategies under increasing abiotic stress

Brooke Vogt[1], Anna Kazarina[1], Jack Sytsma[1], Bryttan Adams[1], Leslie Rodela[1], Dasik Clouse[1], Reece Keller[1], Darcy Thompson[1], Helen Winters[1], Maggie Wagner[2], Sara Baer[2], Ari Jumpponen[1], Loretta Johnson[1], and Sonny T.M. Lee[1*]

[1] Division of Biology, Kansas State University, Manhattan, Kansas, USA

[2] Department of Ecology and Evolutionary Biology and the Kansas Biological Survey, University of Kansas, Lawrence, Kansas, USA

[*] corresponding author

Abstract
Shifts in precipitation patterns pose a significant threat to tallgrass prairies by altering soil microbial communities essential for plant resilience. *Andropogon gerardii*, a key species in tallgrass prairies, spans the North American precipitation gradient. However, it remains unclear to what extent the rhizosphere is affected due to the plant host-environmental interaction. To assess how environmental and host factors shape rhizobiome, we conducted a biogeographical survey of *A. gerardii* across 25 sites within its historical range, and characterized microbial communities from the rhizosphere and adjacent local soil samples using 16S amplicon sequencing. We showed that while geographic location largely structured both rhizosphere and soil communities, regional precipitation emerged as a primary driver of microbial community assembly. We observed distinct microbial divides across the dry, mesic, and wet regions of the North American "arid-humid divide." Importantly, we found the first compelling large-scale evidence that regional precipitation profoundly influenced rhizobiome assembly patterns. In the aridest regions, rhizosphere microbial communities exhibited significantly more predicted stochasticity than the local soil, and had microbial families related to host-benefiting functions. Our study highly suggested enhanced plant host selection for specific microbial variants in response to abiotic stress.

Keywords
Microbiome, Microbial Community Assembly, Host-microbe Interactions, *Andropogon gerardii*, Climate Change, Abiotic Stress

Introduction

Changes in the assembly and function of plant host-associated microbiomes can be influenced by a mosaic of factors, such as abiotic stress induced by climate change[1–4]. Over the past 10,000 years, the tallgrass species *Andropogon gerardii* has evolved genetically distinct varieties based on precipitation (dry, mesic, and wet varieties) across North America[5–9]. Microevolutionary processes have modified these varieties' anatomical and physiological traits, enabling them to survive and thrive in regions with differing precipitation levels, temperatures, and soil physiochemical properties[6,10–12].

Some studies suggest that plant host-associated rhizobiome are specific to the plants' locations, indicating that plants within the same ecotype and across different ecotypes are distinct[13,14]. This view asserts that rhizobiome assembly is more strongly influenced by various local abiotic stresses as well as environmental and soil physiochemical characteristics than by regional similarities in precipitation and climate. Other studies propose that rhizobiomes within the same ecotype are similar across various locations, while those of different ecotypes differ from each other[15,16]. According to this perspective, precipitation-based abiotic stress drives the host plants to select similar microorganisms, resulting in analogous rhizobiome communities within the same precipitation ecotype[17,18]. Prior reciprocal garden experiments[19,20] examining the rhizobiome of the dry, mesic, and wet varieties of *A. gerardii* have supported the idea that host-associated rhizobiomes are influenced by regional precipitation. In these studies, *A. gerardii* recruited rhizospheres similar to those at its native sites, fulfilling the home-field advantage hypothesis[19,20]. If microbial assembly is driven by precipitation-based abiotic stress, then different forms of this stress should lead to the host selecting different specialists. Contradicting hypotheses point to the lack of detailed information on how precipitation-based abiotic stress could impact the rhizobiome of ecotypic varieties.

While the differences among dry, mesic, and wet varieties of *A. gerardii* have developed over thousands of years due to phenotypic plasticity, how quickly their host-associated rhizobiome can adapt to long-term changes in precipitation remains to be seen. The consequences of a rhizbiome's ability to adjust to different forms of precipitation-based abiotic stress are crucial. In this century, the 100th meridian ("arid humid" divide) has shifted eastward, which is predicted to accelerate due to the

compounding effects of climate change[5,21–24]. Understanding the assembly of host rhizobiomes and their vulnerabilities is crucial, mainly because *A. gerardii* constitutes 80% of the biomass in tallgrass prairies[25]. In addition to this, central tallgrass prairies are critically endangered, with only 4.4% remaining in North America[6,8,25–28]. Rapid shifts in precipitation patterns may lead to a decline in *A. gerardii* if their microbiomes are closely linked to local ecological and soil microbial communities, and cannot adapt to long-term precipitation shifts. If *A. gerardii* microbiomes are solely influenced by local conditions, then long-term variations in rainfall could pose a significant threat to the host's health, longevity, and survival.

In this current study, we took the opportunity to evaluate how regional precipitation conditions influence rhizobiome assembly, and analyzed whether the plant host exerts more influence on the associated rhizobiomes in areas of more significant precipitation-based abiotic stress. To understand the composition of the microbial communities of the dry, mesic, and wet varieties of *A. gerardii*, we conducted a biogeographical survey across 25 locations in North America. We performed a 16S rRNA amplicon analysis on the local soil (LS) and plant host-associated rhizobiome (RB). Our study addressed three key questions: I) How do local and regional characteristics influence microbial community composition? II) How does host selection affect rhizobiome composition and diversity compared to local soil, and is biotic filtering consistent across abiotic stress levels? III) How do local soil and rhizobiome communities compare in similarity across different precipitation-related ecotypes?

Methods

Sample collection and preparation

Sample collection took place between May and August 2023. We selected 25 sample locations based on the historical habitats of *A. gerardii*, aiming to represent variations in precipitation, soil physiochemical properties, climate, and phenotypic plasticity across the continental United States (Supplementary Table S1). We collected local soil and rhizosphere samples from six randomly chosen *A. gerardii* plants from each location. We took three replicates from each plant, resulting in 18 local soil and 18

rhizosphere samples per location, and 900 samples (450 local soil and 450 rhizosphere) across all 25 locations.

For rhizosphere samples, we collected soil cores (10 cm deep and 1.25 cm in diameter) near the base of the plant tillers. We picked out roots from the soil cores, and gently shook them to remove any loose soil before placing them into a microcentrifuge tube. Subsequently, we transferred approximately 1 gram of soil, free of roots, into a separate microcentrifuge tube for the local soil sample.

Any excess soil (without roots) from the six plant replicates that were not used for the local soil or rhizobiome analyses were combined and stored in sterile bags to analyze soil physiochemical properties (n=25 samples). The samples were kept in coolers with ice, and were transferred to a -80 °C freezer until further processing.

Molecular processing, 16S rRNA amplicon sequencing and analyses

We extracted local soil and rhizosphere samples using the E.Z.N.A.® Soil DNA Kit (Omega BIO-TEK; Georgia, USA). We followed the protocol with minimal modifications for the local soil samples[29]. The only adjustment made was using glass beads for cell lysis, performed with a Qiagen TissueLyser II (Qiagen; Hilden, Germany) at 30 revolutions per second for 10 minutes. For each of the 25 locations, we extracted three replicates separately, and selected one replicate from each of the six plants based on DNA concentration and quality. The final elution volume for each local soil sample (n = 150) was 100 µL.

The rhizosphere samples required significant modifications to the company protocol to ensure optimal DNA quality and yield. For these samples, we combined three replicates into a single sample during the binding phase of the procedure. Additionally, we used liquid nitrogen to crush the roots into a fine powder, and then lysed the cells using the TissueLyser II for 16 minutes at 30 revolutions per second. Depending on the sample location, we adjusted the final elution volumes for the rhizobiome samples, ranging from 30 µL to 150 µL.

We used the Qubit™ dsDNA Broad-range (BR) DNA quantification kit on a Qubit™ 4 Fluorometer (Thermo Fisher Scientific, Invitrogen™; Massachusetts, USA) to determine the sample gDNA concentration. The quality of the DNA was assessed by measuring the

A260/A280 and A260/A230 ratios on a Nanodrop™ One Spectrophotometer (Thermo Fisher Scientific, Invitrogen™; Massachusetts, USA). After quantifying the DNA, we normalized each sample to a 5 ng/µL concentration with molecular-grade DNA/RNA-free water for sequencing.

The normalized gDNA was sequenced at the Kansas State University Integrative Genomics Facility (https://www.k-state.edu/igenomics/). The DNA amplification was performed using the 515F and 806R primers[30] (16S rRNA v4 amplicon region), and sequenced with 2 x 300 cycles on the Illumina MiSeq (Illumina; California, USA). We utilized QIIME 2 v. 2024.5[31] to process the raw reads. We applied the QIIME 2 cutadapt[32] plugin to remove the primer sequences.

Subsequently, we eliminated sequences with an error rate greater than 0.1 and those with undetermined bases or without a primer. For further quality control, we used DADA2[33] with consistent parameters across various runs to trim the reads, ensuring that the 25th percentile of reads had a quality score below 15 (Forward = 270 and Reverse = 250). We employed the pre-trained classifier in QIIME 2 for bacterial taxonomic classification, referencing the SILVA v. 138 database[34]. To mitigate biases caused by differences in sequence depth across samples in subsequent diversity analyses, we rarefied the dataset to 15,000 reads per sample. Finally, we used the QIIME 2 pipeline to compute alpha and beta diversity metrics. After generating the ASV table, we removed all eukaryotic, unresolved, unclassified at the domain level, all ASVs that contained chloroplasts and mitochondria, and non-specific reads before conducting statistical analyses.

In order to methodically tease apart the influence of environment and pant host on the rhizobiome composition, we performed beta dispersion analyses to examine how community assembly strategies influenced the distance to the centroid between dry and wet local soil and rhizobiome samples, focusing on whether sample distribution was driven more by stochastic (random) or deterministic processes. We defined samples where beta dispersion distances close to 1 indicate unique randomness, while smaller distances (0.8) demonstrate stochastic processes with clearer and more predictable forms of randomness[35].

For oligotyping analysis, we employed the QIIME 2 oligotype function[36] (v. 3.2) and the minimum entropy decomposition algorithm[37] (MED) to identify oligotypes within our aligned 16S rRNA amplicon sequences. We aligned our sequences using the MUSCLE function[38]. To ensure an unbiased taxonomic assessment of oligotypes across various sample types, we set the number of components to 7 with a minimum substantive abundance parameter of 1 and included all features. These parameters were determined based on the entropy analysis of oligotype entropy peaks. We retained (LS: n = 2,248) and (RB: n = 2,876) oligotypes in this analysis.

In our taxonomic evaluation, we extracted specific features belonging to particular families from our previous taxonomic assessment (SILVA v. 138[34]), filtering for features that belonged to the *Micromonosporaceae* and *Pedosphaeraceae* families due to their significant representation and overall abundance across all samples. We set the number of components to 2 for the taxonomic analysis while maintaining a minimum substantive abundance parameter of 1. Following the taxonomic oligotyping analysis, *Micromonosporaceae, Nitrosphaeraceae*, *Xiphinematobacteraceae, Vicinamibacteraceae, Rhodanobacteraceae,* and *Pedosphaeraceae* families yielded the following total number of oligotypes: (LS: n = 9 and RB: n = 10; LS: n = 9 and RB: n = 10; LS: n = 14 and RB: n = 13; LS and RB: n = 16; LS: n = 6 and RB: n = 7; and LS and RB: n = 16).

Soil physiochemical properties

All analyses of soil physicochemical properties were conducted at Kansas State University's Soil Testing Laboratory (https://www.agronomy.k-state.edu/ outreach-and-services/soil-testing-lab/soil-analysis/researchers.html). The analyses were performed on local soil samples (n = 25). Detailed procedures are in the revised version of the Recommended Chemical Soil Test Procedures for the North Central Region manual[39,40]. However, a summary of the methods for each test is provided.

Samples were analyzed for various physiochemical properties, including soil pH, total nitrogen, carbon percentages (both organic and inorganic), phosphorus content, and texture (percentages of sand, silt, and clay). Before analysis, all samples were dried in a

drying oven at 60 °C. Once the soil was arid, it was passed through a 2 mm sieve to break up aggregates and ensure homogeneity.

For pH analysis, 10 grams of soil were mixed with an equal amount of deionized water in a 1:1 solution[39,41–43]. The mixture was stirred for 5 seconds or until a uniform soil-water slurry was achieved. After allowing it to sit for 10 minutes, pH measurements were taken using a Skalar SP50 Robotic Analyzer (Skalar Inc.; Georgia, USA).

Phosphorus concentrations were measured in parts per million (ppm P) using the Mehlich III method on 2 grams of soil[39,44,45]. The soil was suspended in a 1:10 solution with the standard Mehlich III solution, which consists of 0.2 N acetic acid (CH_3COOH), 0.25 N ammonium nitrate (NH_4NO_3), 0.015 N ammonium fluoride (NH_4F), 0.013 N nitric acid (HNO_3), and 0.001 N EDTA (ethylenediaminetetraacetic acid)($HOOCCH_2)_2NCH_2CH_2N(CH_2COOH)_2$). The mixture was shaken at 200 excursions per minute for 5 minutes. After shaking, the slurry was filtered through a Whatman No. 42 filter. From the clear filtered slurry, 2 mL was transferred to a test tube, and 8 mL of the working solution was added. The working solution was prepared by combining 25 mL of Murphy-Riley Solution A (which contains 0.051 N ammonium molybdate [$(NH_4)_6Mo_7O_{24}$•$4H_2O$] and 0.004 N antimony potassium tartrate [$K_2Sb_2(C_4H_2O_6)_2$•$3H_2O$]) with 10 mL of Solution B (0.749 N ascorbic acid [$C_6H_8O_6$]) in a total volume of 1 L.

After letting the mixture sit for 10 minutes, the samples were loaded in triplicate onto a 96-well plate and analyzed using a Lachat QuikChem 8500 Series 2 photometric colorimeter (Hach Inc.; Colorado, USA) at a wavelength of 882 nm, following the orthophosphate method (12-115-01-1-A). Phosphorus measurements were determined by comparing the samples against a 500 ppm potassium dihydrogen phosphate (KH_2PO_4) stock solution, diluted to a 50 ppm standard solution before loading into the 96-well plate.

Total nitrogen and total carbon analyses were conducted on 0.35 grams of soil. The total nitrogen and carbon levels (including organic and inorganic components) were analyzed using a LECO TruSpec CN analyzer (LECO; Michigan, USA), following the procedures outlined in the operation manual[46]. The analysis showed a standard deviation of 2.18% for soil carbon and 3.35% for soil nitrogen. The samples were encapsulated and securely sealed in the loading head. They were then purged to eliminate any atmospheric

gases that could interfere with the measurements. Once all atmospheric gases were removed, the samples were combusted at 950°C to ensure rapid combustion while flushed with pure oxygen. A consistent aliquot of gases was then homogenized and separated. The total percentage of carbon and nitrogen was calculated based on weight percentages using the formula: Total % of Carbon or Nitrogen = (Mass of C or N / Total Sample Mass) * 100.

Soil texture was determined using the modified hydrometer method[47,48] on a 50-gram soil sample. First, the soil was placed in a dispersion cup, and then 100 mL of a 5% sodium hexametaphosphate solution ($Na_6(PO_3)_6$) was added. The mixture was stirred for 30 to 60 seconds until it was uniform. This slurry was then transferred to a 1000 mL cylinder filled to the 1000 mL mark with deionized water. The mixture was allowed to sit overnight to settle. To begin the experiment, a plunger was inserted, and the sample was mixed for an additional 30 seconds to ensure homogeneity. A Bouyoucos hydrometer (Fisherbrand™; Soil Analysis ASTM Hydrometer) was then placed in the slurry. After 40 seconds, the initial hydrometer reading was recorded. A second reading was taken after 2 hours.

The percentages of sand, silt, and clay were calculated using the following formulas: - % Clay = (Final Reading * 100 / mass of sample) - % Silt = (Initial Reading * 100 / mass of sample) - % Clay - % Sand = 100% - % Silt - % Clay All readings were adjusted using a blank sample (100 mL of the 5% dispersion solution plus 880 mL of deionized water) and applying temperature and density corrections. For every one °F above 68 °F, 0.2 was added to the reading, while for every one °F below 68 °F, 0.2 was subtracted from the reading.

Statistical analyses and data visualization

We used RStudio version 4.4.2[49,50] for all statistical analyses and figure generation. We defined significance for all tests as having a p-value less than 0.05. For our studies of soil properties, we utilized the car[51], devtools[52], dunn.test[53], pairwiseAdonis[54], and vegan[55] packages to evaluate how unique the soil's physicochemical properties were based on the sample's location, precipitation depth, and precipitation ecotype.

We conducted one-way ANOVA analyses to assess factors such as soil pH, phosphorus concentration (ppm P), carbon and nitrogen content (% total C and N), C:N ratio, soil texture (% sand, % silt, and % clay), and precipitation depth concerning the sample location and precipitation-ecotype (dry, mesic, and wet). Following this, we performed a Tukey HSD post hoc test to identify and classify the group means, particularly where statistical differences were noted from the ANOVA analysis. Additionally, we applied Kruskal-Wallis rank sum tests to evaluate pairwise comparisons between sample locations and ecotypes for both the local soil and rhizobiome samples to analyze our soil properties and precipitation depth. Finally, we conducted PERMANOVA analyses to determine whether bacterial community composition varied based on location, precipitation ecotype, soil properties, and precipitation depth, followed by PERMANOVA pairwise comparisons to explore the interactions between locations, ecotypes, soil properties, and precipitation depth on community composition.

We analyzed the alpha diversity metrics, sample location, ecotype, and pH/precipitation depth gradients using a one-way ANOVA to compare the means of the number of observed features (Sobs), Faith's phylogenetic diversity (Faith's PD), and Shannon's entropy (H') for the local soil and rhizobiome samples. We performed two-way ANOVA to analyze the relationship between our alpha diversity metrics, ecotypes, and pH/precipitation depth. Following the ANOVA, we performed a Tukey HSD post hoc test to identify and classify the group means. Additionally, we performed Kruskal-Wallis rank sum tests for the same alpha diversity metrics to evaluate pairwise comparisons between sample locations and ecotypes for the local soil and rhizobiome samples. We used linear regression to analyze statistically significant changes to microbial abundances across our pH and precipitation gradients.

To calculate and analyze the distance between the ecotypes' centroids and confirm the trends observed in the heatmaps, we conducted beta diversity dispersion (betadisper) analyses. Using the car[51] and vegan[55] packages, we assessed the differences between groups based on the mean distance to the centroid for each group. This evaluation helped us determine the probability of overlap between the ecotypes. Within our betadisper test, we performed the PERMANOVA, a permutation, and a pairwise permutation test to examine sample heterogeneity within each ecotype. Finally,

we used Pearson's Chi-squared tests in the tidyverse[56] and readr[57] packages to find statistical differences in ASV composition between sample types (LS and RB) and the associated ecotypes.

We used beta dispersion distances and the beta-group-significance function in QIIME 2 to infer stochasticity within a location between sample types to surmise the underlying strategies of community assembly. We then used a one-way ANOVA to define statistical differences among the beta dispersion means for each location and sample type. For the oligotyping analysis, we used the beta dispersion tests described previously.

We utilized the RStudio packages ggplot2[58], patchwork[59], dplyr[60], multcomp[61], multcompView[62], agricolae[63], tidyr[64], venn[65], tidyverse[56], vegan[55], cluster[66], sf[67], maps[68], reshape2[69], pheatmap[70], RColorBrewer[71], car[51], gridExtra[72], phyloseq[73], igraph[74], ggnewscale[75], readr[57], ggthemes[76], ggtext[77], ggVennDiagram[78], randomcoloR[79], stringr[80], and VennDiagram[81] to visualize the analyses performed in this study. All bioinformatic and R codes are deposited in GitHub (https://github.com/SonnyTMLee/Plant-host-identity-drives-rhizobiome-assembly-under-increasing-abiotic-stress.git).

Results and Discussion

We processed a total of 13,087,481 (local soil) and 16,677,859 (rhizobiome) raw reads. After quality control, we retained 11,759,436 reads (2,462 ASVs) for the local soil and 14,627,083 reads (3,039 ASVs) for the rhizobiome. In the local soil samples, 92% (2,267 ASVs) of the ASVs resolved to the genus level, and 64% (1,567 ASVs) resolved to the species level. We observed similar resolution across the rhizobiome samples, where 93% (2,815 ASVs) resolved to the genus and 65% (1,985 ASVs) resolved to the species level. The five most abundant phyla in the local soil samples were Proteobacteria (22%, 532 ASVs), Actinobacteriota (11%, 278 ASVs), Bacteroidota (9.8%, 242 ASVs), Chloroflexi (8.1%, 200 ASVs), and Acidobacteriota (7.6%, 187 ASVs). We observed similar dominant phyla across the rhizobiome samples, with Proteobacteria (23%, 691 ASVs) being the most dominant, followed by Actinobacteriota (10%, 315 ASVs), Bacteroidota (9.9%, 302 ASVs), Planctomycetota (7.5%, 229 ASVs), and Chloroflexi

(7.5%, 228 ASVs) (Supplementary Table S2). Of all our samples, 0.12% (3 ASVs) from the local soil and 0.13% (4 ASVs) from the rhizobiome were unclassified.

Regional precipitation shaped both local soil and plant host-associated microbial communities

We used non-metric multidimensional scaling (NMDS) and optimal silhouette scores from k-means clustering, and identified two distinct clusters among the local soil (silhouette score = 0.21) and rhizobiome (silhouette score = 0.22) samples (Figure 1A, 1B). We observed that regional precipitation patterns significantly influenced the two identified clusters - "wet-associated ecotype" and "dry-associated ecotype". Samples in the transition zone (overlap) between the wet and dry associated ecotypes were categorized as "mesic-associated ecotype." The ten samples classified as dry-associated ecotypic local soil (DAE_{LS}) were: MT1, SD1, ND1, MN1, CO1, KS2, NM1, NE2, OK1, and TX3. Three samples (KS1, NE1, and IA1) belonged to the mesic-associated ecotypic local soil (MAE_{LS}), and 12 samples (WI1, MI1, IN1, MO1, IL1, TX1, TX2, LA1, AL1, NC1, and SC1) were categorized as wet-associated ecotypic local soil (WAE_{LS}). The dry-associated ecotypic local soil had the same assignments as the dry-associated ecotypic rhizobiome (DAE_{RB}). However, the sample assignments exhibited slight changes from the local soil for the mesic (MAE_{RB}) and wet (WAE_{RB}) ecotypic rhizobiome, in which IA1 and NE1, were reclassified into the WAE_{RB} category in the rhizobiome. We surmised that the dry-associated ecotype had more stable sample assignments than the wet or mesic-associated ecotypes due to long-lasting relationships between the dry variety of *A. gerardii* and its associated rhizobiome[6,19,82]. In contrast, the wet and mesic-associated ecotypes have more heterogeneity, possibly due to the shifting of historical precipitation boundaries, bringing aridity to historically moist locations for centuries[24,83,84]. This change was most striking as a result of the acceleration of eastward shifts of regional precipitation zones encompassing the 100th meridian, with predictive models foreshadowing accelerations of these transitions within this century[24].

In order to provide insights into the impact of regional precipitation on the local soil and rhizobiome composition, we used the NOAA[85] database for precipitation depth data, selected the maximum precipitation depth over 60 days at the sample locations, and

mapped the distribution of our clustering analysis across the precipitation gradient (Figure 1C). We observed a clear divide between the clustered dry and wet ecotypes, which resembled distinct points along the 100th meridian, often called the "arid-humid divide." The clustering of our samples within the regions of the 100th meridian suggests that large-scale precipitation patterns can significantly influence the composition of microbiomes across geographically diverse locations[86]. This indicates that the selective pressures exerted by precipitation may surpass the effects of local climate, geographic, and soil property differences[87,88].

We used one-way ANOVA analysis, and showed statistical significance between the associated ecotypes and their precipitation depth (LS: $p < 2.2 * 10^{-16}$ and RB: $p < 2.2 * 10^{-16}$; Precipitation: DAE_{LS} = 221.5 ± 46.2 mm and DAE_{RB} = 224.3 ± 45.7 mm, MAE_{LS} = 312.4 ± 15.0 mm and MAE_{RB} = 325.1 ± 0 mm, and WAE_{LS} = 360.9 ± 55.9 mm, and WAE_{RB} = 350.5 ± 54.864 mm). Kruscal-Wallis post hoc pairwise tests showed that for the local soil, the precipitation depth between the DAE_{LS} and the WAE_{LS} was most significant (p-adj = 3.92×10^{-20}), followed by the DAE_{LS} vs. MAE_{LS} (p-adj = 3.34×10^{-5}) and WAE_{LS} vs. MAE_{LS} (p-adj = 1.02×10^{-1}). This trend was also observed for the rhizobiome samples DAE_{RB} vs. WAE_{RB} (p-adj = 2.08×10^{-9}), DAE_{RB} vs. MAE_{RB} (p-adj = 4.08×10^{-2}), and WAE_{RB} vs. MAE_{RB} (p-adj = 1.00).

We further used PERMANOVA, and showed a significant impact of precipitation depth on local soil and rhizobiome community structures ($p = 0.001$). Pairwise PERMANOVA tests also indicated that all interactions between the community composition, associated ecotypes, and precipitation depth for the local soil were significant (adj p-values = 0.003 for all pairwise comparisons). However, though PERMANOVA pairwise analysis showed significantly different bacterial composition between the DAE_{RB} and WAE_{RB}, (adj p-value = 0.003), comparisons between WAE_{RB} and MAE_{RB} as well as DAE_{RB} and MAE_{RB} were insignificant (adj p-values = 0.16 and 0.07, respectively). Our results corroborated with another study[20], showing that regional precipitation influences local soil communities more than the plant host-associated rhizobiome communities. Here, we demonstrated the influence and regulation due to the plant host from adverse hydrologic conditions on its associated rhizobiome community

structure[1,89,90]. Next, we wanted to ask if and to what extent physiochemical soil properties contributed to this variation.

Soil physiochemical properties and bacterial diversity were primarily influenced by geographic location rather than regional precipitation

We analyzed soil physiochemical properties - soil pH, total nitrogen (% TN), total carbon (% TC), phosphorus content (ppm P), carbon-to-nitrogen ratios (C:N), and soil texture (% sand, % silt, % clay) at the 25 locations.

We observed that the soil physiochemical properties were more closely related to location than our associated precipitation ecotypes (Figure 2A). All soil properties were statistically significant between the locations (Supplementary Table S3), but only soil pH (LS: $p = 1.05 \times 10^{-12}$), sand content (LS: $p = 1.02 \times 10^{-2}$), and silt content (LS: $p = 1.90 \times 10^{-4}$) from associated precipitation ecotypes were significantly different from each other. We postulate that the lack of significant differences within our community-defined ecotypes arose because the extreme variability of individual local soil properties in specific locations was mitigated, resulting in comparable soil characteristics over extensive regions[91].

Our results suggested that local soil communities were significantly influenced by soil pH ($DAE_{LS} = 7.00 \pm 0.74$, $MAE_{LS} = 7.27 \pm 0.71$, $WAE_{LS} = 6.17 \pm 0.64$; Kruskal-Wallis: DAE_{LS} vs. WAE_{LS} ($p = 5.40 \times 10^{-8}$), the DAE_{LS} vs. MAE_{LS} ($p = 0.02$), and the WAE_{LS} vs. MAE_{LS} ($p = 1.60 \times 10^{-5}$), whereas in the rhizobiome, root exudates from the host plant could act as buffers to maintain pH homeostasis[92]. Although, in the rhizobiome, the only significant difference from our PERMANOVA pairwise analysis was observed between the DAE_{RB} and WAE_{RB}, ($p = 0.003$), suggesting that increased rainfall in the wetter regions could have led to the leaching of basic cations from the soil, resulting in a lower pH; while soils with limited rainfall retained these cations, making them more alkaline[93].

Our findings further indicated that the ratio (PD:pH) between precipitation depth (PD) and soil pH was significant in the local soil and rhizobiome across the associated ecotypes ($p = 0.001$). The precipitation depth and pH ratio were significant for all local soil-associated ecotypes ($p = 0.003$) for all interactions (Supplementary Table S3). However, for the rhizobiome, only the interaction between the DAE_{RB} and WAE_{RB} was

significant ($p = 0.003$). The relationships intertwining soil pH, precipitation, and bacterial diversity are complicated. While pH and precipitation emerged as primary drivers of change in bacterial diversity[94,95], the extent to which these two variables directly influenced bacterial community composition remained unclear[94,95]. However, common trends regarding pH and precipitations' impacts on specific microbial alpha diversity indices have been well documented[86,87,95,96], leading us to investigate these relationships.

We observed that, across the 25 locations, alpha diversity metrics were significantly tied to locations (ANOVA: (LS: Sobs $p = 1.06 \times 10^{-8}$, Faith PD $p = 4.91 \times 10^{-10}$, and H' $p = 7.38 \times 10^{-10}$) and (RB: Sobs $p = 6.56 \times 10^{-6}$, Faith $p = 4.54 \times 10^{-8}$, and H' $p = 1.98 \times 10^{-5}$)) (Figure 2B). On the other hand, while local soil alpha diversity metrics were significant across the local soil-associated ecotypes (ANOVA: (LS: Sobs $p = 6.02 \times 10^{-5}$, Faith PD $= 1.55 \times 10^{-3}$, and H' $p = 8.75 \times 10^{-6}$)); there was no significance between the rhizobiome samples possibly due to shielding from the host (Supplementary Table S3).

We examined how pH and precipitation gradients influenced the organization of our associated ecotypes in terms of microbial diversity and abundance. We found that precipitation depth significantly affected all alpha diversity metrics across (ANOVA: LS and RB (Sobs $p = 0.05$, Faith PD $p = 3.82 * 10^{-3}$, H' $p = 7.17 * 10^{-3}$) and between the sample types (LS vs. RB) ($p < 2 * 10^{-16}$) (Figure 2D, S1). Pairwise tests further revealed that the most dramatic differences in diversity were observed between the following precipitation categories across sample types: (H': (LS: p-adj $= 2.21 * 10^{-3}$ (pH 9 to pH 9.5 vs. pH 12.5 to pH 13), RB: p-adj $= 3.21 * 10^{-3}$ (pH 6.5 to pH 7 vs. pH 15 to pH 15.5)); Sobs: (LS: p-adj $= 2.05 * 10^{-3}$ (pH 9 to pH 9.5 vs. pH 12.5 to pH 13), RB: p-adj $= 3.99 * 10^{-3}$ (pH 6.5 to pH 7 vs. pH 16.5 to pH 17)); and Faith PD: (LS: p-adj $= 2.21 * 10^{-3}$ (pH 13 to pH 13.5 vs. pH 16.5 to pH 17), RB: p-adj $= 6.05 * 10^{-4}$ (pH 14 to pH 14.5 vs. pH 16.5 to pH 17)) (Figure 2E, 2F). While the alpha diversity metrics in our study were more stable across categories of increased precipitation[97], the local soil revealed the most substantial differences in alpha diversity, mainly among moderate precipitation categories, while the rhizobiome displayed more variable changes, especially between extreme precipitation groups. This suggests that soil microbial communities were more responsive to subtle deviations in precipitation depth within our “mesic buffer zone” separating arid and moist

areas[97,98]. However, because of the mitigating effects of the host, the rhizobiome appeared to be more resistant to intermediate precipitation fluctuations, only showing differences among precipitation extremes[99].

Linear regression analysis revealed significant changes of relative abundance across the precipitation gradient for seven phyla: *Crenarchaeota*, *Desulfobacterota*, *MBNT15*, *Planctomycetota*, *RCP2-54*, *Verrucomicrobiota*, and *WPS-2* with p-values of $p = 4.00 * 10^{-2}$, $p = 1.00 * 10^{-2}$, $p = 9.41 * 10^{-3}$, $p = 2.11 * 10^{-2}$, $p = 1.09 * 10^{-2}$, $p = 3.46 * 10^{-4}$, and $p = 9.64 * 10^{-4}$ representatively (Figure S2). All except *Crenarchaeota* (slope = $-1.22 * 10^{-4}$; $R^2 = 0.306$) increased in relative abundance with greater precipitation depth. We hypothesize that the decrease in *Crenarchaeota* might be due to their roles as ammonia-oxidizing archaea (AOA), which might not be in high demand or feasible under waterlogged conditions[100].

In contrast, no significant changes in alpha diversity (ANOVA: (Sobs p = 0.73, Faith PD = 0.59, H' p = 0.49)) or bacterial relative abundance were found across the pH gradient; with significant changes only observed when comparing sample types ($p < 2 * 10^{-16}$) and ecotype regarding Faith PD ($p = 2.08 * 10^{-3}$) (Figure 2C, S1). However, two-way ANOVA revealed significance regarding the relationship between Shannon diversity and pH*associated ecotype ($p = 1.54 * 10^{-2}$). Additionally, pairwise analysis showed no significant differences in alpha diversity metrics between rhizobiome categories, and minimal significance in local soil pH categories across all metrics. The minimal variations seen among the pH categories and bacterial diversity suggested that the legacy of the host plant could significantly influence present microbe-plant cohabitation[10,101,102]. Our previous reciprocal garden experiment[19] also supported this hypothesis, where the rhizobiomes of the wet varieties planted in dry soil had lower richness (Sobs) than mesic and dry varieties in the same soil. Collaborating with our previous findings that precipitation is the most critical factor in driving differences in host-associated rhizobiome composition under "abiotic extremes" led us to ask the following question: How does the interaction between precipitation, sample type, and associated ecotype influence the distribution of ASVs among our samples?

Bacterial community composition revealed patterns that differentiated associated ecotypes

We observed that the local soil and rhizobiome samples had similar microbial community composition trends across and within our associated ecotypes (Figure 3A). Interestingly, we observed that the dry-associated ecotypes had community compositions more similar to each other than the wet-associated ecotypes, suggesting that increased abiotic stress might have a filtering effect on the microbial community structures[103,104].

We showed that both the dispersion of each associated ecotype (BetaDisper distance to median: (DAE_{LS} = 0.33 and DAE_{RB} = 0.30; MAE_{LS} = 0.21 and MAE_{RB} = 0.20; and WAE_{LS} = 0.33 and WAE_{RB} = 0.34)) for the local soil and the rhizobiome were significant (PERMANOVA, p = 0.001; F-statistic LS: 28.4 and RB: 24.9). Furthermore pairwise comparisons showed that all interactions (DAE_{LS} vs. MAE_{LS}: $p = 1.57 \times 10^{-13}$, MAE_{LS} vs. WAE_{LS}: $p = 1.35 \times 10^{-9}$; DAE_{RB} vs. MAE_{RB}: $p = 1.75 \times 10^{-7}$, MAE_{RB} vs. WAE_{RB}: $p = 4.79 \times 10^{-6}$, and DAE_{RB} vs. WAE_{RB}: $p = 1.00 \times 10^{-3}$); except one interaction (DAE_{LS} vs. WAE_{LS}: p = 0.91), were significant between the associated ecotypes. These results corroborated with our previous findings that the microbial communities within each ecotype could vary significantly, with some associated ecotypes showing more significant heterogeneity (dry and wet) than others (mesic)[19]. Although there are no statistical differences between the dry and the wet associated ecotypes, the following scenarios prompted us to investigate differences in ecotypic microbial composition: I) We noticed that the dry rhizobiome samples are more similar to each other than dry local soil; II) Additionally, the dry rhizobiome composition is very different from the wet rhizobiome (Figure 3B). While the shared ASVs across all associated ecotypes (41.2% LS and 34.4% RB) represented the highest relative abundance, the wet-associated ecotype had the second-highest number of unique ASVs (20.1% LS and 23.8% RB), followed by the dry-associated ecotype (15.3% LS and 11.9% RB) (Figure 3C). Across the sample types (LS and RB), we observed that 26.5% of ASVs were shared among all ecotypes and samples (Figure 3D), with the wet having more unique ASVs than the dry ecotype. We deduce that this difference could be linked to various microbial legacy effects and adaptation to abiotic stress[105,106]. In this context, the dry ecotype might prefer specialist microbes over

generalists, reducing the overall number of unique ASVs[107,108]. Correspondingly, the minor number of unique ASVs between ecotypes and sample types might result from phylogenetic divergence and variations in niche space where microbes adapted to specific precipitation pressures that may not suit contrasting environments[109]. We further confirmed that there were significant differences in unique ASVs across ecotypes (Chi-squared, $p = 2.2 \times 10^{-16}$), and between wet and dry ecotypes ($p = 0.05$), demonstrating that differences in unique ASVs were primarily due to ecotype, but not sample type. Our results implied that complex environmental and ecotypic factors had a more profound impact on shaping the number of unique ASVs than the localized effects of the individual plant host.

Stochastic processes influenced community composition more in local soil than in rhizobiome in arid locations

Both local soil and rhizobiome samples showed high beta dispersion distances across all of our locations and associated ecotypes, common among grassland microbiomes (Figure 4A, 4B)[110]. We observed notable differences between the dry ecotypic local soil and rhizobiome communities, in which 8 out of 10 comparisons showed significant differences in beta dispersion (Dry: TX3: $p = 3.43 \times 10^{-5}$, NE1: $p = 5.41 \times 10^{-6}$, OK1: $p = 1.45 \times 10^{-11}$, KS2: $p = 3.08 \times 10^{-2}$, ND1: $p = 1.20 \times 10^{-3}$, MT1: $p = 6.02 \times 10^{-3}$, SD1: $p = 5.06 \times 10^{-3}$, NM1: $p = 1.52 \times 10^{-3}$, and CO1: $p = 8.69 \times 10^{-4}$), whereas only one comparison for wet-associated ecotypes was significant (Wet: MI1: $p = 3.02 \times 10^{-2}$). Notably, among the two driest locations, CO1 and NM1, the local soil had significantly higher beta dispersion than their rhizobiome communities, a trend unique to dry-associated ecotypes. We hypothesize that dispersal limitation and host influence on microhabitat stability and selection might drive the observed differences in stochasticity among various sample types in the driest locations. This could result from dry ecotypes reducing dispersal effects by fostering specialized microbial communities shaped by abiotic stress, leading to a more stable rhizobiome community structure than the local soil[111]. With the dry-associated ecotypic rhizobiome demonstrating less stochasticity, we next asked what microbial populations in the rhizobiome could contribute to the similarity and stability associated with the dry ecotypic plant hosts.

Oligotyping analysis reveals contrasting variant compositions across ecotypes and sample types for two prokaryotic families

To analyze fine-scale ecological patterns in local soil and rhizobiome samples across wet and dry ecotypes, we conducted an unbiased taxonomic oligotype assessment for all our ASVs. Our clustering for oligotyping analysis mirrored the clustering of our ASVs, suggesting that there was a limited impact of rare oligotypes within each taxon from each location, as well as precipitation and ecological pressures driving common trends between ASVs and their variants at each location (Figure S3).

For both sample types, the permutation test for homogeneity revealed significant differences in dispersion between the associated ecotypes for each sample type (LS and RB: $p = 0.001$, LS: $F = 10.9$, RB: $F = 14.2$). However, we only observed differences between the dry and wet ecotypes within the rhizobiome ((LS distance to centroid: 0.24 and 0.26, $p = 0.13$) and (RB distance to centroid: 0.21 and 0.26, $p = 4.25 * 10^{-6}$) for dry and wet, respectively) (Figure 5A). The distinctions between dry and wet rhizobiomes could originate from more substantial selection pressures and reduced microbial diversity at our drier locations. Furthermore, the contrast between dry local soil and rhizobiome might be more pronounced due to host selection[112], microhabitat stabilization[113], and environmental filtering[107].

Given the differences between the dry and wet ecotypes and across the two sample types, we aimed to evaluate the oligotypic patterns within specific ASV families to examine the abundance of particular community oligotypes among closely related species of microorganisms (Figure 5B). Taxonomic analysis revealed distinct results across the ecotypes and sample types among the *Micromonosporaceae, Nitrosphaeraceae*, and *Xiphinematobacteraceae* versus the *Vicinamibacteraceae, Rhodanobacteraceae,* and *Pedosphaeraceae* families. For the *Micromonosporaceae, Niteosphaeraceae*, and *Xiphinematobacteraceae* families, the highest relatively abundant oligotypes in the local soil differed significantly from those in the rhizobiome, with very few “core” variants between sample types. The similarities between the dry and wet rhizobiome oligotypes compared to the local soil suggested that host selection might favor specific oligotypes over others[114], regardless of the location and variant composition of

the local soil for members of the *Micromonosporaceae* family. This observed host influence might stem from notably, that many species in the *Micromonosporaceae* family are frequently associated with plant rhizospheres due to their production of plant growth regulators, including auxins and gibberellins[115,116]. Additionally, the *Nitrosphaeraceae* family constitutes ammonia-oxidizing archaea (AOA), which may benefit host nutrient acquisition[117]. The fact that both of these families had similar oligotypic distribution patterns supported the "stress-induced selection" hypothesis, where under abiotic stress, plants would likely retain the microorganisms within the rhizobiome that benefit the plant[118,119].

However, in the *Vicinamibacteraceae, Rhodanobacteraceae,* and *Pedosphaeraceae* families, there was greater similarity of oligotypes across ecotypes and sample types, indicating a more extensive variety of "core" variants (Figure 4E). While more shared oligotypes existed, each location was more distinct than observed in the *Micromonosporaceae* family. We speculated that these differences arised because members of the *Pedosphaeraceae* family are more "free-living" than those associated with the *Micromonosporaceae* family[120]. Because of this minimized host selection, its local soil and rhizobiome oligotype composition were more similar within a location, meaning that the oligotypes found in the rhizobiome most likely originated from the local soil, with little to no host filtering[113,114].

Despite these apparent distinctions among these families, common trends emerged. Generally, the wet local soil and rhizobiome contained more oligotypes than the dry local soil and rhizobiome locations, reflecting on the filtering effect from both the environment and plant host[121,122]. Additionally, the rhizobiome consistently had more oligotypes than the local soil, suggesting that the plant host could support a higher diversity of microorganisms within a family due to increased nutrients and reduced fluctuating-associated stress. Additionally, we theorized that microhabitat stability and the increased number of features present for the rhizobiome in both families (*Micromonosporaceae*: LS: n = 329 and RB: n = 587; *Xiphinematobacteraceae:* LS: n = 251 and RB: n = 305; *Nitrosphaeraceae:* LS: n = 196 and RB: n = 205; *Vicinamibacteraceae:* LS: n = 758 and RB: n = 932; *Rhodanobacteraceae:* LS: n = 136 and RB: n = 318; *Pedosphaeraceae*: LS: n = 755 and RB: n = 1,083) might have

contributed to the rhizobiome samples having more variants regardless of ecotype[123]. Considering the oligotypic analysis here, we suggest that as the abiotic stress of the environment increases, the host influence on the rhizobiome community exerts a greater pressure.

Conclusion

Precipitation and climate conditions significantly shape the compositions of microbiome communities[124]. However, discrepancies between precipitation depth and the strength of host interaction can lead to varying impacts on community structure, some of which can be exacerbated under increased abiotic stress[125,126]. Here, we demonstrated that regional precipitation profoundly affected and categorized *A. gerardii* into three distinct associative ecotypes, i.e., dry, mesic, and wet associative ecotypes. Notably, the geographic span of our associative ecotypes crossed distinguishable areas of the 100th meridian, known as North America's “arid-humid divide.” We speculate that our associated ecotypes' composition and geographic span might be linked to the *A. gerardii* host varieties' diversity and legacy effects[9,12,127]. Additionally, our findings showed that although pH and precipitation depth had a more pronounced effect on local soil than on rhizobiome communities, alterations in rhizobiome diversity were more pronounced at precipitation extremes. We surmise that these differences might arise from host ecotypic effects through microhabitat stabilization. By stratifying our samples by type and respective ecotypes, we further identified large-scale trends in microbial community composition, particularly in the differences between the dry and wet associative ecotypes. In this study, we observed significant variations in the relative abundances of specific phyla belonging to specific sample type-associated ecotypes. This suggests specialized roles of specific phylum responding to precipitation-related stress and underscores potential rainfall-community structure relationships.

Furthermore, for the first time, we showed notable differences in rhizobiome and local soil microbial diversity with reduced precipitation, revealing possible links between abiotic stress and microbial community assembly strategies (stochastic vs. deterministic). We further showed that regional precipitation was a critical factor in ecotypic rhizobiome assembly, with the rhizosphere communities in the aridest locations exhibiting more

predicted forms of randomness than the local soil, implying plant host-associated biotic filtering under extreme abiotic stress (Figure 6). Our findings highlighting the shift toward reduced stochasticity in the ecotypic microbial communities under intensified abiotic stress underscores the pivotal role of regional precipitation in shaping plant-associated rhizobiome, and suggests that plant hosts might rely heavily on biotic filtering mechanisms to mitigate extreme environmental challenges.

Funding
This study is supported by the United States Department of Agriculture, National Institute of Food and Agriculture (USDA NIFA), project award (Number 2020-67019-3180) and the National Science Foundation CAREER Award (Number 2238633) as well as by the National Science Foundation Award (Number OIA-1656006) with matching support from the State of Kansas through the Kansas Board of Regents.

Acknowledgments
We thank everyone involved in sampling and data acquisition; this research would not have been possible without your contributions. We also thank Tanner Riche and Qinghong Ran for their helpful discussions on data analysis. We appreciate the work conducted by Alina Akhunova, Jose Ruiz Ortiz, and Samantha Elledge at the Integrated Genomic Facility at Kansas State University (https://www.k-state.edu/igenomics/). In addition, we thank the Kansas State University Soil Testing Laboratory for helping with the soil property analyses (https://www.agronomy.k-state.edu/outreach-and-services/soil-testing-lab/).
We acknowledge that this research was conducted on land that is the historical homeland of many Native Nations, who have long served as stewards of North American tallgrass prairies. We honor their histories, cultures, and traditions and recognize their contributions to the ecological and historical knowledge of tallgrass prairie ecosystems.

Conflicts of Interest
The authors stated no conflicts of interest.

Author Contributions
A.K., J.S., D.C., H.W., M.W., S.B., A.J., L.J., and S.T.M.L. collected and processed samples. B.V., B.A., L.R., R.K., D.C., and D.T. extracted, quantified, and normalized genomic DNA. B.V. and A.K. conducted the bioinformatic analysis of 16S rRNA sequencing. B.V. carried out the statistical analyses. B.V. and S.T.M.L. authored the manuscript, developed figures, and prepared all supplementary files. A.J. and L.J. assisted with revisions of the manuscript and figures. S.T.M.L., A.J., L.J., M.W. and S.B. secured funding for this study. All authors reviewed, edited, and endorsed the last version of this manuscript.

Author's Information

Sonny T.M. Lee:
X: @sonnytmlee
Bluesky: @sonnytmlee.bsky.social
LinkedIn: https://www.linkedin.com/in/sonny-tm-lee-a25b9120
ResearchGate: https://www.researchgate.net/profile/Sonny-Lee-3

Brooke Vogt:
X: @VogtBrookeM

Bluesky: @brookevogt.bsky.social
LinkedIn: www.linkedin.com/in/brooke-vogt-5a351035b
ResearchGate: https://www.researchgate.net/profile/Brooke-Vogt

Figures

Figure 1: ***Precipitation-associated sample clustering and geospatial analysis***

(A) NMDS clustering of local soil samples with k-means clustering and optimized silhouette scores showing distinct groupings with 95% confidence ellipses. Each point represents a sample, colored according to NOAA's 60-day maximum precipitation depth at the collection site.

(B) NMDS clustering of rhizobiome samples with the same clustering criteria. Sample points are uniquely marked and colored by precipitation depth, consistent with part A.

(C) Map of biogeographical survey sites, with markers colored by NOAA's 60-day maximum precipitation depth. Stacked bar graphs within the map display the proportion of local soil samples assigned to each NMDS-defined group at each site. The adjacent pie charts summarize group assignments for rhizobiome samples.

Figure 2: ***Ecotypic soil physiochemical properties and alpha diversity across associated ecotypes and soil property gradients***

(A) Violin plots showing the distribution of soil physicochemical properties across assigned local soil ecotypes (dry-, mesic-, and wet-associated). Statistical differences among ecotypes were assessed using ANOVA with Tukey's HSD post hoc tests. Red, green, and blue panels represent dry, mesic, and wet ecotypes, respectively.

(B) Alpha diversity metrics, including observed features, Shannon entropy, and Faith's PD, are grouped by associated ecotype for local soil and rhizobiome samples. Significance was evaluated in the same manner as in part A. Red, green, and blue panels represent dry, mesic, and wet ecotypes, respectively.

(C) Comparison of alpha diversity metrics between local soil and rhizobiome samples across environmental pH categories (assessed using independent t-tests. Statistical significance is indicated as follows: ns (grey) = $p > 0.05$, * (orange) $p < 0.05$, ** (red) $p < 0.01$, *** (brown) $p < 0.001$.

(D) Comparison of alpha diversity metrics between local soil and rhizobiome samples across precipitation depth (PD) categories, also assessed in the same manner as in part C.

Statistical significance is indicated as follows: ns (grey) = $p > 0.05$, * (orange) $p < 0.05$, ** (red) $p < 0.01$, *** (brown) $p < 0.001$.

Figure 3: ***Beta diversity patterns and ASV distribution across associated ecotypes and sample types***

(A) Bray–Curtis dissimilarity heatmaps illustrating large-scale community composition trends in (A) local soil and (B) rhizobiome samples, clustered by their associated ecotypes.

(B) PCoA plots of beta dispersion, showing community variability within associated ecotypes for each sample type. The accompanying box plots display the distance of each sample to the group centroid.

Statistical significance is defined as follows: ns = $p > 0.05$, * $p < 0.05$, ** $p < 0.01$, *** $p < 0.001$.

(C) Venn diagrams depicting the distribution of shared and unique ASVs across associated ecotypes for local soil and rhizobiome samples.

(D) Combined Venn diagram comparing ASV overlap between local soil and rhizobiome sample types across all associated ecotypes.

Figure 4: ***Within-site community variability across local soil and rhizobiome samples***

(A) Beta dispersion analysis of local soil samples, assessing within-site variability across locations. Sample points are colored by their associated ecotype, with lines representing the mean distance to the centroid for each ecotype and shaded bars indicating standard deviation. Sites are arranged in order of decreasing precipitation depth.

(B) Beta dispersion analysis of rhizobiome samples, with sample coloring and site arrangement as described in part A.

Statistical comparisons between local soil and rhizobiome samples at each site indicate significant differences in beta dispersion, suggesting variation in community stochasticity across sample types.

Statistical significance is denoted as follows: ns = $p > 0.05$, * $p < 0.05$, ** $p < 0.01$, *** $p < 0.001$.

Figure 5: ***Community variant structure and oligotype composition across associated ecotypes and sample types***

(A) PCoA plots of beta dispersion based on taxonomically unbiased oligotyping analysis, illustrating community variability within associated ecotypes for each sample type. Accompanying box plots display the distance of individual samples to their group centroid, describing within-group variability. Statistical significance is denoted as follows: ns = $p > 0.05$, * $p < 0.05$, ** $p < 0.01$, *** $p < 0.001$.

(B) The top panels represent host-selected communities. Stacked bar plots showing the relative abundance (y-axis) of individual oligotypes within selected prokaryotic families, stratified by sample type and dry- versus wet-associated ecotypes (x-axis). Each color corresponds to a distinct oligotype variant. Details of the oligotypes are in Supplementary Tables 10 and 11.

(C) Oligotypes of microbial populations hypothesized to be non-host-selected communities. Stacked bar plots showing the relative abundance (y-axis) of individual oligotypes within selected prokaryotic families, stratified by sample type and dry- versus wet-associated ecotypes (x-axis). Each color corresponds to a distinct oligotype variant. Details of the oligotypes are in Supplementary Tables 10 and 11.

Figure 6: ***Conceptual model summarizing the influence of precipitation-driven abiotic stress on soil and rhizobiome community assembly***

The top panel illustrates a subdivision of the United States precipitation gradient, highlighting two locations, A and B, to describe two scenarios based on our findings.

The second panel (Location A) illustrates a high-stress environment with limited precipitation. In this scenario, plant host selection strongly influences rhizobiome community assembly, resulting in divergence from the surrounding soil community and the enrichment of specialist taxa. This shift reflects reduced environmental influence and increased host-mediated filtering under abiotic stress. Here, the stochasticity of the rhizobiome becomes more uniform as site aridity increases while the local soil remains highly variable.
In contrast, the bottom panel (Location B) depicts a low-stress environment characterized by high precipitation. Under these conditions, environmental influences dominate, while the impact of plant hosts is minimal. Consequently, local soil and rhizobiome communities are highly variable. Generalist taxa dominate both communities. Here, the stochasticity of the local soil and rhizobiome remains highly unstable, and precipitation has a minimal effect.

Supplementary Figures

Figure S1: ***Microbial community composition across climated and soil property gradients***

Stacked bar plots showing the relative abundance of ASVs classified at the phylum level, stratified by associated ecotype, environmental pH categories (first), and precipitation depth (second) gradients. This visualization highlights compositional shifts in microbial communities along climate and soil property gradients.

Figure S2: ***Linear regression analysis of phylum-level microbial abundance across ecotypes and sample types with increasing precipitation depth***

Linear models assessed phyla whose relative abundances significantly correlated with precipitation depth across different ecotypes and sample types (local soil and rhizobiome). Only phyla exhibiting significant relationships with precipitation ($p < 0.05$) are shown, highlighting taxa potentially responsive to moisture variability along the precipitation gradient.

Figure S3: ***Taxonomically Unbiased Oligotype Clustering***

NMDS taxonomically unbiased oligotype clustering of local soil (first) and rhizobiome (second) variants within each sample with k-means clustering and optimized silhouette scores showing distinct groupings with 95% confidence ellipses. Each point represents a sample, colored according to NOAA's 60-day maximum precipitation depth at the collection site.

Supplementary Tables

Table S1: Site Locations with Precipitation Metrics

Table S2: QIIME Local Soil and Rhizobiome Sequences Before and After Quality Trimming

Table S3: Soil Properties and Alpha Diversity Statistical Analyses

Table S4: ASV Assignments for the Local Soil and Rhizobiome Samples

Table S5: Soil Chemistry

Table S6: Alpha Diversity for the Local Soil and Rhizobiome Samples

Table S7: ASV Distribution by Sample Type and Associated Ecotype

Table S8: Beta Dispersion Distance for Local Soil and Rhizobiome Samples within a Location

Table S9: Precipitation and pH Gradient t-Test Results

Table S10: Unbiased Taxonomic Oligotyping Results

Table S11: Oligotyping Results for Individual Families

References

1. Bandopadhyay, S., Li, X., Bowsher, A. W., Last, R. L. & Shade, A. Disentangling plant- and environment-mediated drivers of active rhizosphere bacterial community dynamics during short-term drought. *Nat. Commun.* **15**, 6347 (2024).
2. Bei, Q., Moser, G., Wu, X., Müller, C. & Liesack, W. Metatranscriptomics reveals climate change effects on the rhizosphere microbiomes in European grassland. *Soil Biol. Biochem.* **138**, 107604 (2019).
3. Direct and indirect effects of climate change on soil microbial and soil microbial-plant interactions: What lies ahead? doi:10.1890/ES15-00217.1.
4. Zeglin, L. H. *et al.* Altered precipitation regime affects the function and composition of soil microbial communities on multiple time scales. *Ecology* **94**, 2334–2345 (2013).
5. Axelrod, D. I. Rise of the Grassland Biome, Central North America. *Bot. Rev.* **51**, 163–201 (1985).
6. Maricle, B. R., Caudle, K. L., Lindsey, K. J., Baer, S. G. & Johnson, L. C. Effects of Extreme Drought on Photosynthesis and Water Potential of Andropogon gerardii (Big Bluestem) Ecotypes in Common Gardens Across Kansas. *tkas* **120**, 1–16 (2017).
7. Kramer, D. L. *et al.* Drought tolerance in ecotypes of big bluestem (Andropogon gerardii) relates to above-ground surface area: Results from a common garden experiment. *Flora* **246-247**, 52–60 (2018).
8. Galliart, M. *et al.* Adaptive genetic potential and plasticity of trait variation in the foundation prairie grass Andropogon gerardii across the US Great Plains' climate gradient: Implications for climate change and restoration. *Evol. Appl.* **13**, 2333–2356 (2020).
9. Mendola, M. L., Baer, S. G., Johnson, L. C. & Maricle, B. R. The role of ecotypic variation and the environment on biomass and nitrogen in a dominant prairie grass. *Ecology* **96**, 2433–2445 (2015).
10. Olsen, J. T., Caudle, K. L., Johnson, L. C., Baer, S. G. & Maricle, B. R. Environmental and

genetic variation in leaf anatomy among populations of Andropogon gerardii (Poaceae) along a precipitation gradient. *Am. J. Bot.* **100**, 1957–1968 (2013).

11. Barnes, P. W. Adaptation to Water Stress in the Big Bluestem-Sand Bluestem Complex. *Ecology* **66**, 1908–1920 (1985).
12. Johnson, L. C. *et al.* Intraspecific variation of a dominant grass and local adaptation in reciprocal garden communities along a US Great Plains' precipitation gradient: implications for grassland restoration with climate change. *Evol. Appl.* **8**, 705–723 (2015).
13. Wang, X.-B. *et al.* Habitat-specific patterns and drivers of bacterial β-diversity in China's drylands. *ISME J.* **11**, 1345–1358 (2017).
14. Cai, Z., Wang, X., Bhadra, S. & Gao, Q. Distinct factors drive the assembly of quinoa-associated microbiomes along elevation. *Plant Soil* **448**, 55–69 (2020).
15. Alegria Terrazas, R. *et al.* A footprint of plant eco-geographic adaptation on the composition of the barley rhizosphere bacterial microbiota. *Sci. Rep.* **10**, 12916 (2020).
16. Pang, Z., Xu, P. & Yu, D. Environmental adaptation of the root microbiome in two rice ecotypes. *Microbiol. Res.* **241**, 126588 (2020).
17. Marasco, R. *et al.* Rhizosheath microbial community assembly of sympatric desert speargrasses is independent of the plant host. *Microbiome* **6**, 215 (2018).
18. Cowan, D. A. *et al.* Biogeographical survey of soil microbiomes across sub-Saharan Africa: structure, drivers, and predicted climate-driven changes. *Microbiome* **10**, 131 (2022).
19. Kazarina Anna *et al.* Home-field advantage affects the local adaptive interaction between Andropogon gerardii ecotypes and root-associated bacterial communities. *Microbiology Spectrum* **11**, e00208–23 (2023).
20. Sarkar, S. *et al.* Bacterial but Not Fungal Rhizosphere Community Composition Differ among Perennial Grass Ecotypes under Abiotic Environmental Stress. *Microbiol Spectr* **10**, e0239121 (2022).
21. Seager, R. *et al.* Projections of declining surface-water availability for the southwestern

United States. *Nat. Clim. Chang.* **3**, 482–486 (2012).

22. Seager, R. *et al.* Dynamical and Thermodynamical Causes of Large-Scale Changes in the Hydrological Cycle over North America in Response to Global Warming. *J. Clim.* **27**, 7921–7948 (2014).
23. Cook, B. I., Smerdon, J. E., Seager, R. & Coats, S. Global warming and 21st century drying. *Clim. Dyn.* **43**, 2607–2627 (2014).
24. Seager, R. *et al.* Whither the 100th meridian? The once and future physical and human geography of America's arid–humid divide. Part II: The meridian moves east. *Earth Interact.* **22**, 1–24 (2018).
25. Knapp, A. K., Briggs, J. M., Blair, J. M. & Turner, C. L. Patterns and controls of aboveground net primary production in tallgrass prairie. *Grassland dynamics: long-term ecological research in tallgrass prairie. Oxford University Press, New York* 193–221 (1998).
26. Fred B. Samson, Fritz L. Knopf, and Wayne R. Ostlie. Great Plains ecosystems: past, present, and future. *Wildlife Society Bulletin* **32**, 6–15 (2004).
27. Ren, Z. *et al.* The role of dominant prairie species ecotypes on plant diversity patterns of restored grasslands across a rainfall gradient in the US Great Plains. *Appl. Veg. Sci.* **26**, (2023).
28. Hoekstra, J. M., Boucher, T. M., Ricketts, T. H. & Roberts, C. Confronting a biome crisis: global disparities of habitat loss and protection. *Ecol. Lett.* **8**, 23–29 (2005).
29. Omega Bio-tek, Inc, Norcross, GA, USA. E.Z.N.A.® Soil DNA Kit (Revision No: 1.3).
30. Caporaso, J. G. *et al.* Ultra-high-throughput microbial community analysis on the Illumina HiSeq and MiSeq platforms. *ISME J.* **6**, 1621–1624 (2012).
31. Bolyen, E. *et al.* Reproducible, interactive, scalable and extensible microbiome data science using QIIME 2. *Nat. Biotechnol.* **37**, 852–857 (2019).
32. Martin, M. Cutadapt removes adapter sequences from high-throughput sequencing reads. *EMBnet J.* **17**, 10 (2011).

33. Callahan, B. J. *et al.* DADA2: High-resolution sample inference from Illumina amplicon data. *Nat. Methods* **13**, 581–583 (2016).

34. Quast, C. *et al.* The SILVA ribosomal RNA gene database project: improved data processing and web-based tools. *Nucleic Acids Res.* **41**, D590–6 (2013).

35. Cao, P. *et al.* Environmental filtering process has more important roles than dispersal limitation in shaping large-scale prokaryotic beta diversity patterns of grassland soils. *Microb. Ecol.* **72**, 221–230 (2016).

36. Eren, A. M. *et al.* Oligotyping: Differentiating between closely related microbial taxa using 16S rRNA gene data. *Methods Ecol. Evol.* **4**, 1111–1119 (2013).

37. Eren, A. M. *et al.* Minimum entropy decomposition: unsupervised oligotyping for sensitive partitioning of high-throughput marker gene sequences. *ISME J.* **9**, 968–979 (2015).

38. Edgar, R. C. MUSCLE: multiple sequence alignment with high accuracy and high throughput. *Nucleic Acids Res.* **32**, 1792–1797 (2004).

39. Combs, S. M. and Nathan, M. V. *Recommended Chemical Soil Test Procedures for the North Central Region North Central Regional*. vol. 211 (Reised) (University of Missouri Agricultural Experiment Station, Columbia, MO, 1998).

40. Dakota, S. Recommended Chemical Soil Test Procedures for the North Central Region. (1998).

41. Watson, M. pH and lime requirement.

42. Mclean, E. O. Soil pH and Lime Requirement. in *Agronomy Monographs* 199–224 (American Society of Agronomy, Soil Science Society of America, Madison, WI, USA, 2015). doi:10.2134/agronmonogr9.2.2ed.c12.

43. Brown, J. R. & Cisco, J. R. An improved Woodruff buffer for estimation of lime requirements. *Soil Sci. Soc. Am. J.* **48**, 587–592 (1984).

44. Mehlich, A. Mehlich 3 soil test extractant: A modification of Mehlich 2 extractant. *Commun. Soil Sci. Plant Anal.* **15**, 1409–1416 (1984).

45. Murphy, J. & Riley, J. P. A modified single solution method for the determination of phosphate in natural waters. *Anal. Chim. Acta* **27**, 31–36 (1962).
46. LECO Corporation, St. Joseph, MI. Carbon and Nitrogen in Soil and Sediment. (2005).
47. Foth, H.D., H.S. Jacobs, and L.V. Withee. Laboratory Manual for Introductory Soil Science, 3rd Ed. 12–13 (1971).
48. Bouyoucos, G. J. Hydrometer method improved for making particle size analysis of soils. *Agron. J.* **54**, 464–465 (1962).
49. RStudio Team. RStudio: Integrated Development for R. RStudio. *PBC* (2024).
50. R Core Team. R: A language and environment for statistical computing. *R Foundation for Statistical Computing, Vienna, Austria* (2024).
51. J. Fox, S. W. *An R Companion to Applied Regression, 3rd Ed*. (SAGE Publications, Thousand Oaks, CA, 2019).
52. Chang, H. W. J. H. *devtools: Tools to Make Developing R Packages Easier*, R package version 2.4.3. (2021).
53. Dinno, A. dunn.test: Dunn's Test of Multiple Comparisons Using Rank Sums. R package version 1.3.5. (2017).
54. Arbizu, F. *pairwiseAdonis: Pairwise Multilevel Comparison Using Adonis*, R package version 0.4. (2020).
55. J. Oksanen, F.G. Blanchet, M. Friendly, et al. vegan: Community Ecology Package R package version 2.5-7. (2020).
56. Wickham et al., H. Welcome to the Tidyverse. *J. Open Source Softw.* **4**, 1686 (2019).
57. Hadley Wickham and Jim Hester and Jennifer Bryan. readr: Read Rectangular Text Data. *R package version 2.1.5* (2024).
58. Wickham, H. ggplot2: Elegant Graphics for Data Analysis. *Springer-Verlag New York* (2016).
59. Pedersen, T. L. patchwork: The Composer of Plots. *R package version 1.2.0* (2024).

60. H. Wickham, R. François, L. Henry, K. Müller. *dplyr: A Grammar of Data Manipulation*, R package version 1.0.7. (2021).
61. Bretz, W. T. H. Simultaneous Inference in General Parametric Models. *Biometrical Journal* **50**, 346–363 (2008).
62. R. Graves, F. Piepho, L. Selzer, A. Dorai-Raj. *multcompView: Visualizations of Paired Comparisons*, R package version 0.1-8. (2019).
63. de Mendiburu, F. *agricolae: Statistical Procedures for Agricultural Research*, R package version 1.3-5. (2020).
64. Hadley Wickham and Davis Vaughan and Maximilian Girlich. tidyr: Tidy Messy Data. *R package version 1.3.1*.
65. Dusa, A. venn: Draw Venn Diagrams. *R package version 1.12* (2024).
66. Martin Maechler and Peter Rousseeuw and Anja Struyf and Mia Hubert and Kurt Hornik. cluster: Cluster Analysis Basics and Extensions. (2023).
67. Pebesma, E. J. Simple Features for R: Standardized Support for Spatial Vector Data. *R J.* **10**, 439–446 (2018).
68. Becker, R.A., Wilks, A.R., Brownrigg, R., Minka, T.P., & Deckmyn, A. *maps: Draw Geographical Maps*. R package version 3.3.0. (2018).
69. Wickham, H. Reshaping Data with the {reshape} Package. *Journal of Statistical Software* **21**, 1–20 (2007).
70. Kolde, R. *pheatmap: Pretty Heatmaps*, R package version 1.0.12. (2017).
71. Neuwirth, E. RColorBrewer: ColorBrewer Palettes, R package version 1.1-2. (2014).
72. Auguie, B. gridExtra: Miscellaneous Functions for ‘Grid’ Graphics. R package version 2.3. (2017).
73. P. J. McMurdie, S. H. Phyloseq: An R Package for Reproducible Interactive Analysis and Graphics of Microbiome Census Data. *PLoS One* **8**, e61217 (2013).
74. G. Csardi, T. N. The igraph software package for complex network research. *InterJournal*

1695, (2006).

75. Campitelli, D. *ggnewscale: Multiple Fill and Colour Scales in 'ggplot2'*, R package version 0.4.5. (2021).
76. Arnold, J. B. ggthemes: Extra Themes, Scales and Geoms for 'ggplot2'. *R package version 5.1.0* (2024).
77. Claus O. Wilke and Brenton M. Wiernik. ggtext: Improved Text Rendering Support for 'ggplot2'. *R package version 0.1.2* (2022).
78. Dusa, C.-H. G. A. ggVennDiagram: A 'ggplot2' Implement of Venn Diagram. *R package version 1.5.2* (2024).
79. Ammar, R. randomcoloR: Generate Attractive Random Colors. **R packageersion 1.1.0.1**, (2019).
80. Wickham, H. stringr: Simple, Consistent Wrappers for Common String Operations. *R package version 1.5.1* (2023).
81. Chen, H., & Boutros, P.C. VennDiagram: A package for the generation of highly-customizable Venn and Euler diagrams in R. *BMC Bioinformatics* **12**, (2011).
82. Yang, C. *et al.* Influence of plant genotype and soil on the cotton rhizosphere microbiome. *Front. Microbiol.* **13**, 1021064 (2022).
83. Easterling, D. R. *et al.* Precipitation change in the United States. (2017).
84. Seager, R. *et al.* Whither the 100th meridian? The once and future physical and human geography of America's arid–humid divide. Part I: The story so far. *Earth Interact.* **22**, 1–22 (2018).
85. St. Laurent M. Trypaluk C. Unruh D. Martin D. & Wilhite O., P. S. P. S. *NOAA Atlas 14 Volume 11 Version 2: Precipitation-Frequency Atlas of the United States, Northeastern States*. *NOAA* (2020).
86. Walters, K. E. & Martiny, J. B. H. Alpha-, beta-, and gamma-diversity of bacteria varies across habitats. *PLoS One* **15**, e0233872 (2020).

87. Zhang, Q. *et al.* Alpha, beta and gamma diversity differ in response to precipitation in the Inner Mongolia grassland. *PLoS One* **9**, e93518 (2014).

88. Yao, M. *et al.* The differentiation of soil bacterial communities along a precipitation and temperature gradient in the eastern Inner Mongolia steppe. *Catena* **152**, 47–56 (2017).

89. Chen, P. *et al.* Water management-mediated changes in the rhizosphere and bulk soil microbial communities alter their utilization of urea-derived carbon. *Microorganisms* **12**, 1829 (2024).

90. Vieira, S. *et al.* Drivers of the composition of active rhizosphere bacterial communities in temperate grasslands. *ISME J.* **14**, 463–475 (2020).

91. Orwin, K. H. *et al.* Linkages of plant traits to soil properties and the functioning of temperate grassland: Links of plant traits to soil properties. *J. Ecol.* **98**, 1074–1083 (2010).

92. Badri, D. V. & Vivanco, J. M. Regulation and function of root exudates. *Plant Cell Environ.* **32**, 666–681 (2009).

93. Rengel, Z. Role of pH in availability of ions in soil. *Handbook of plant growth pH as the master variable* (2002) doi:10.1201/9780203910344-20/role-ph-availability-ions-soil-zdenko-rengel.

94. Tan, W., Wang, J., Bai, W., Qi, J. & Chen, W. Soil bacterial diversity correlates with precipitation and soil pH in long-term maize cropping systems. *Sci. Rep.* **10**, 6012 (2020).

95. Zhou, Z., Wang, C. & Luo, Y. Meta-analysis of the impacts of global change factors on soil microbial diversity and functionality. *Nat. Commun.* **11**, 3072 (2020).

96. Rousk, J. *et al.* Soil bacterial and fungal communities across a pH gradient in an arable soil. *ISME J.* **4**, 1340–1351 (2010).

97. Li, J., Benti, G., Wang, D., Yang, Z. & Xiao, R. Effect of alteration in precipitation amount on soil microbial community in a semi-arid grassland. *Front. Microbiol.* **13**, 842446 (2022).

98. Li, X., Yan, Y., Lu, X., Fu, L. & Liu, Y. Responses of soil bacterial communities to precipitation change in the semi-arid alpine grassland of Northern Tibet. *Front. Plant Sci.*

13, 1036369 (2022).

99. Bhattacharyya, A. *et al.* Rhizosphere plant-microbe interactions under water stress. *Adv. Appl. Microbiol.* **115**, 65–113 (2021).

100. Nicol, G. W. & Schleper, C. Ammonia-oxidising Crenarchaeota: important players in the nitrogen cycle? *Trends Microbiol.* **14**, 207–212 (2006).

101. Sutherland, J., Bell, T., Trexler, R. V., Carlson, J. E. & Lasky, J. R. Host genomic influence on bacterial composition in the switchgrass rhizosphere. *Mol. Ecol.* **31**, 3934–3950 (2022).

102. Galliart, M. *et al.* Local adaptation, genetic divergence, and experimental selection in a foundation grass across the US Great Plains' climate gradient. *Glob. Chang. Biol.* **25**, 850–868 (2019).

103. Lucas, J. A. *et al.* Structural and functional study in the rhizosphere of Oryza sativa L. plants growing under biotic and abiotic stress. *J. Appl. Microbiol.* **115**, 218–235 (2013).

104. Hartman, K. & Tringe, S. G. Interactions between plants and soil shaping the root microbiome under abiotic stress. *Biochem. J.* **476**, 2705–2724 (2019).

105. Ginnan, N. A. *et al.* Persistent legacy effects on soil metagenomes facilitate plant adaptive responses to drought. *bioRxivorg* (2024) doi:10.1101/2024.08.26.609769.

106. Hannula, S. E. *et al.* Persistence of plant-mediated microbial soil legacy effects in soil and inside roots. *Nat. Commun.* **12**, 5686 (2021).

107. Metze, D. *et al.* Microbial growth under drought is confined to distinct taxa and modified by potential future climate conditions. *Nat. Commun.* **14**, 5895 (2023).

108. Xie, J. *et al.* Drought stress triggers shifts in the root microbial community and alters functional categories in the microbial gene pool. *Front. Microbiol.* **12**, 744897 (2021).

109. Waring, B. & Hawkes, C. V. Ecological mechanisms underlying soil bacterial responses to rainfall along a steep natural precipitation gradient. *FEMS Microbiol. Ecol.* **94**, fiy001 (2018).

110. Richter-Heitmann, T. *et al.* Stochastic dispersal rather than deterministic selection explains

the spatio-temporal distribution of soil bacteria in a temperate grassland. *Front. Microbiol.* **11**, 1391 (2020).

111. Evans, S., Martiny, J. B. H. & Allison, S. D. Effects of dispersal and selection on stochastic assembly in microbial communities. *ISME J.* **11**, 176–185 (2017).

112. Naylor, D., DeGraaf, S., Purdom, E. & Coleman-Derr, D. Drought and host selection influence bacterial community dynamics in the grass root microbiome. *ISME J.* **11**, 2691–2704 (2017).

113. Albright, M. B. N. *et al.* Interactions of microhabitat and time control grassland bacterial and fungal composition. *Front. Ecol. Evol.* **7**, 447321 (2019).

114. Staley, C. *et al.* Urea amendment decreases microbial diversity and selects for specific nitrifying strains in eight contrasting agricultural soils. *Front. Microbiol.* **9**, 634 (2018).

115. Boukhatem, Z. F., Merabet, C. & Tsaki, H. Plant growth promoting Actinobacteria, the most promising candidates as bioinoculants? *Front. Agron.* **4**, 849911 (2022).

116. Trujillo, M. E., Riesco, R., Benito, P. & Carro, L. Endophytic Actinobacteria and the interaction of Micromonospora and nitrogen fixing plants. *Front. Microbiol.* **6**, 1341 (2015).

117. Sim, J. X. F. *et al.* Pesticide effects on nitrogen cycle related microbial functions and community composition. *Sci. Total Environ.* **807**, 150734 (2022).

118. Millar, N. S. & Bennett, A. E. Stressed out symbiotes: hypotheses for the influence of abiotic stress on arbuscular mycorrhizal fungi. *Oecologia* **182**, 625–641 (2016).

119. Muhammad, A. *et al.* Exploring plant-microbe interactions in adapting to abiotic stress under climate change: a review. *Front. Plant Sci.* **15**, 1482739 (2024).

120. Chen, W.-C., Ko, C.-H., Su, Y.-S., Lai, W.-A. & Shen, F.-T. Metabolic potential and community structure of bacteria in an organic tea plantation. *Appl. Soil Ecol.* **157**, 103762 (2021).

121. Schmidt, V. T. *et al.* Oligotyping reveals community level habitat selection within the genus Vibrio. *Front. Microbiol.* **5**, 563 (2014).

122. Eren, A. M. *et al.* A single genus in the gut microbiome reflects host preference and specificity. *ISME J.* **9**, 90–100 (2015).

123. Giongo, A., Arnhold, J., Grunwald, D., Smalla, K. & Braun-Kiewnick, A. Soil depths and microhabitats shape soil and root-associated bacterial and archaeal communities more than crop rotation in wheat. *Front. Microbiomes* **3**, 1335791 (2024).

124. Dastogeer, K. M. G., Tumpa, F. H., Sultana, A., Akter, M. A. & Chakraborty, A. Plant microbiome–an account of the factors that shape community composition and diversity. *Curr. Plant Biol.* **23**, 100161 (2020).

125. Tripathi, B. M. *et al.* Trends in taxonomic and functional composition of soil microbiome along a precipitation gradient in Israel. *Microb. Ecol.* **74**, 168–176 (2017).

126. Naidoo, Y., Valverde, A., Pierneef, R. E. & Cowan, D. A. Differences in precipitation regime shape microbial community composition and functional potential in Namib Desert soils. *Microb. Ecol.* **83**, 689–701 (2022).

127. Gray, M. M. *et al.* Ecotypes of an ecologically dominant prairie grass (Andropogon gerardii) exhibit genetic divergence across the U.S. Midwest grasslands' environmental gradient. *Mol. Ecol.* **23**, 6011–6028 (2014).

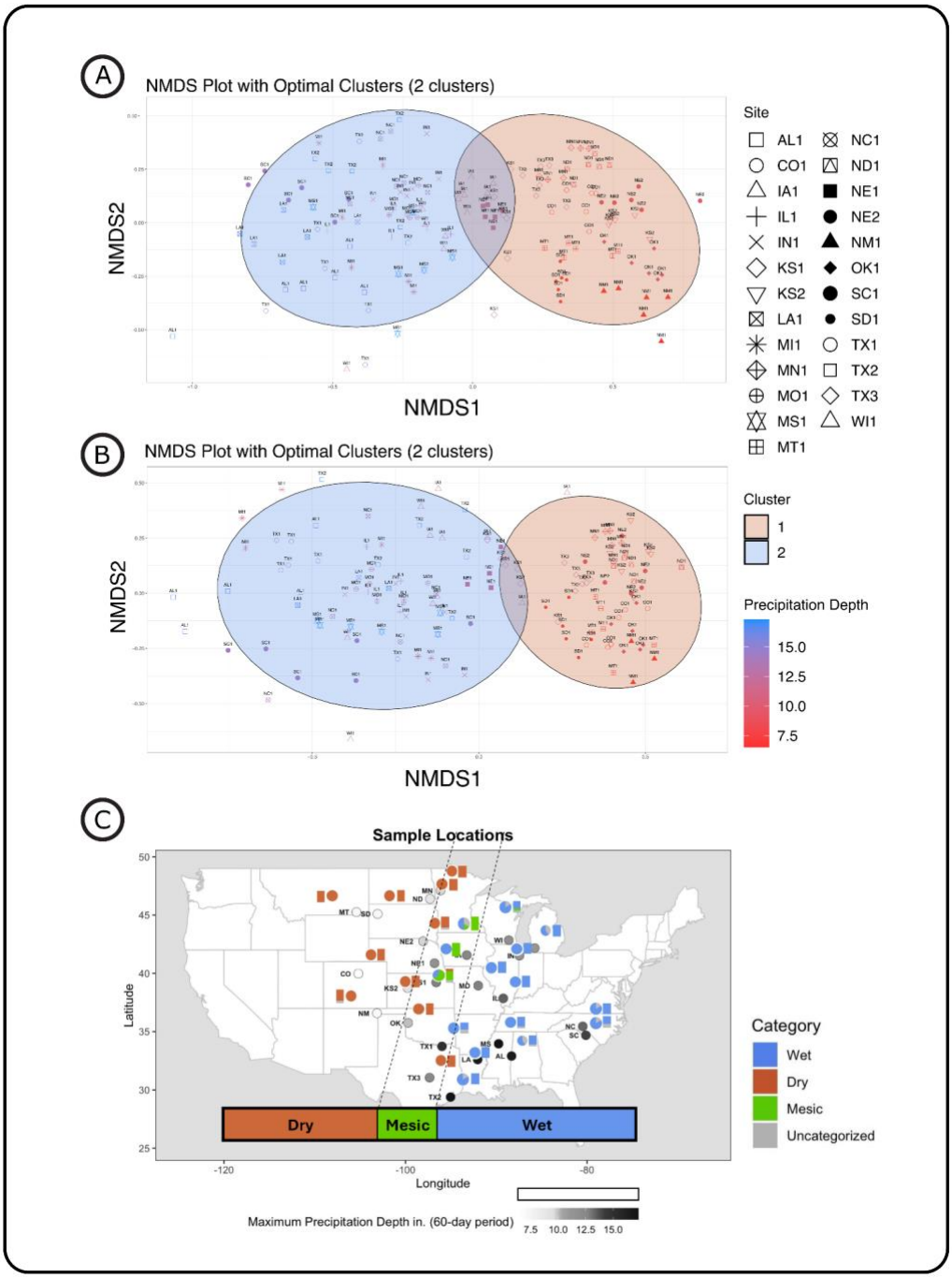
A
NMDS Plot with Optimal Clusters (2 clusters)
NMDS2
NMDS1
Site
AL1
CO1
IA1
IL1
IN1
KS1
KS2
LA1
MI1
MN1
MO1
MS1
MT1
NC1
ND1
NE1
NE2
NM1
OK1
SC1
SD1
TX1
TX2
TX3
WI1
B
NMDS Plot with Optimal Clusters (2 clusters)
NMDS2
NMDS1
Cluster
1
2
Precipitation Depth
15.0
12.5
10.0
7.5
C
Sample Locations
Latitude
Longitude
Dry
Mesic
Wet
Category
Wet
Dry
Mesic
Uncategorized
Maximum Precipitation Depth in. (60-day period)
7.5 10.0 12.5 15.0

Figure 1

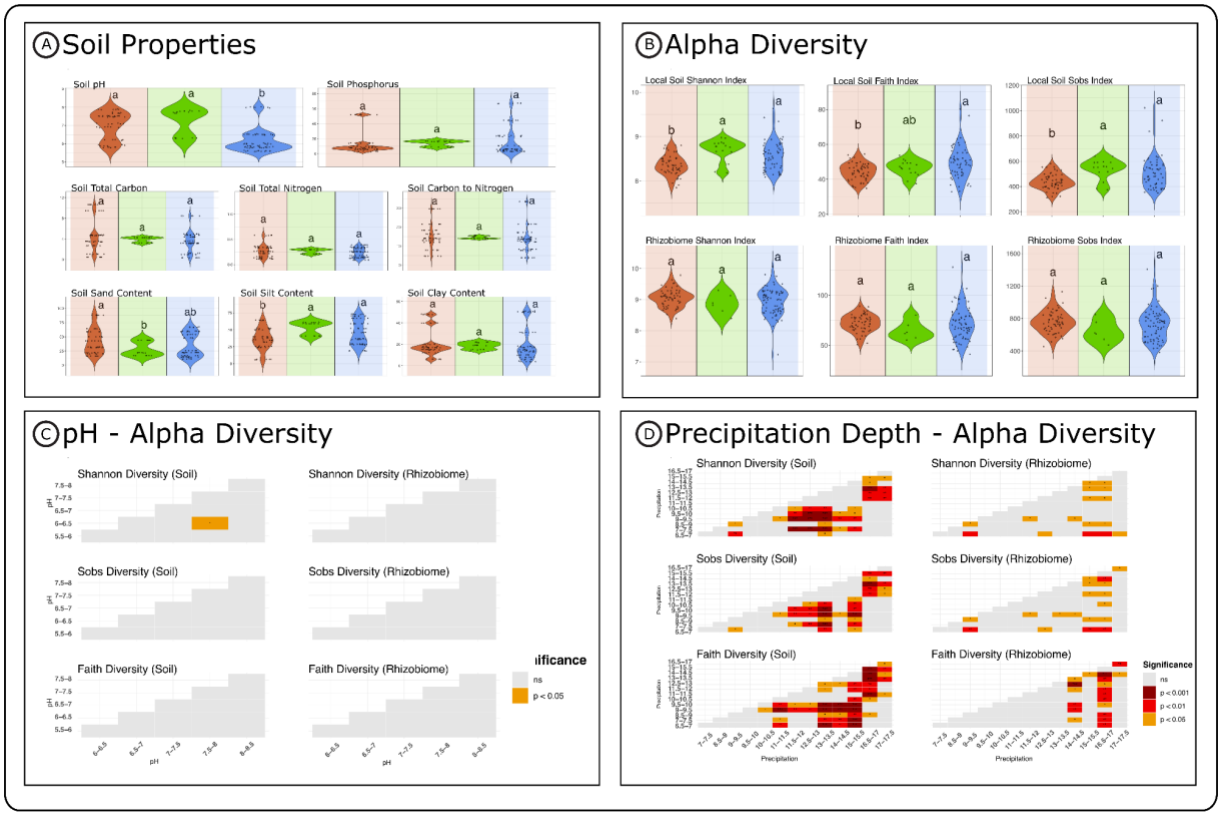
Ⓐ Soil Properties
Soil pH
Soil Phosphorus
Soil Total Carbon
Soil Total Nitrogen
Soil Carbon to Nitrogen
Soil Sand Content
Soil Silt Content
Soil Clay Content
Ⓑ Alpha Diversity
Local Soil Shannon Index
Local Soil Faith Index
Local Soil Sobs Index
Rhizobiome Shannon Index
Rhizobiome Faith Index
Rhizobiome Sobs Index
Ⓒ pH - Alpha Diversity
Shannon Diversity (Soil)
Shannon Diversity (Rhizobiome)
Sobs Diversity (Soil)
Sobs Diversity (Rhizobiome)
Faith Diversity (Soil)
Faith Diversity (Rhizobiome)
ns
p < 0.05
Ⓓ Precipitation Depth - Alpha Diversity
Shannon Diversity (Soil)
Shannon Diversity (Rhizobiome)
Sobs Diversity (Soil)
Sobs Diversity (Rhizobiome)
Faith Diversity (Soil)
Faith Diversity (Rhizobiome)
Significance
ns
p < 0.001
p < 0.01
p < 0.05

Figure 2

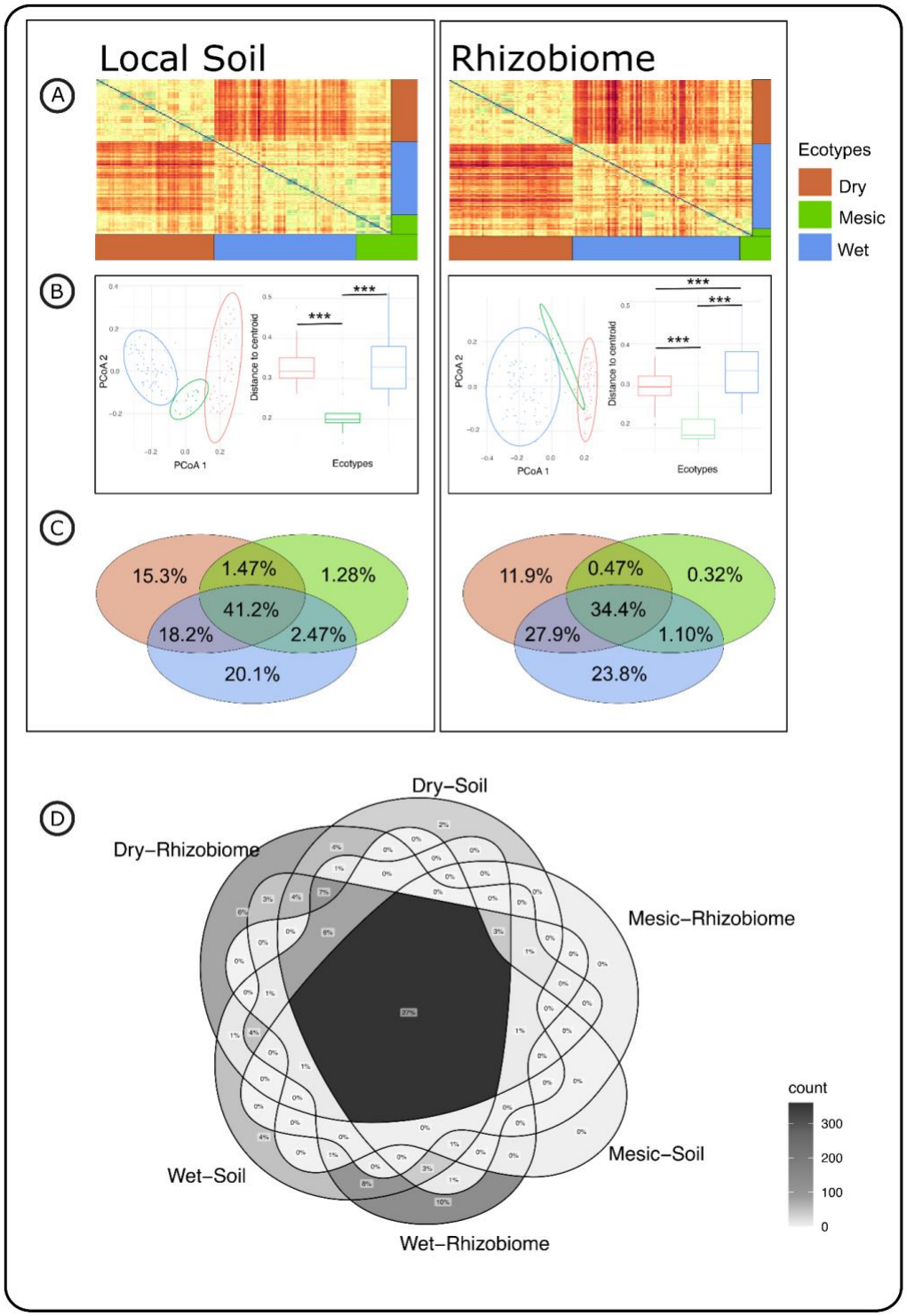
Local Soil
Rhizobiome
A
B
C
D
Ecotypes
Dry
Mesic
Wet
PCoA 2
PCoA 1
Distance to centroid
Ecotypes
***
15.3%
1.47%
1.28%
41.2%
18.2%
2.47%
20.1%
11.9%
0.47%
0.32%
34.4%
27.9%
1.10%
23.8%
Dry−Soil
Dry−Rhizobiome
Mesic−Rhizobiome
Mesic−Soil
Wet−Soil
Wet−Rhizobiome
count
300
200
100
0

Figure 3

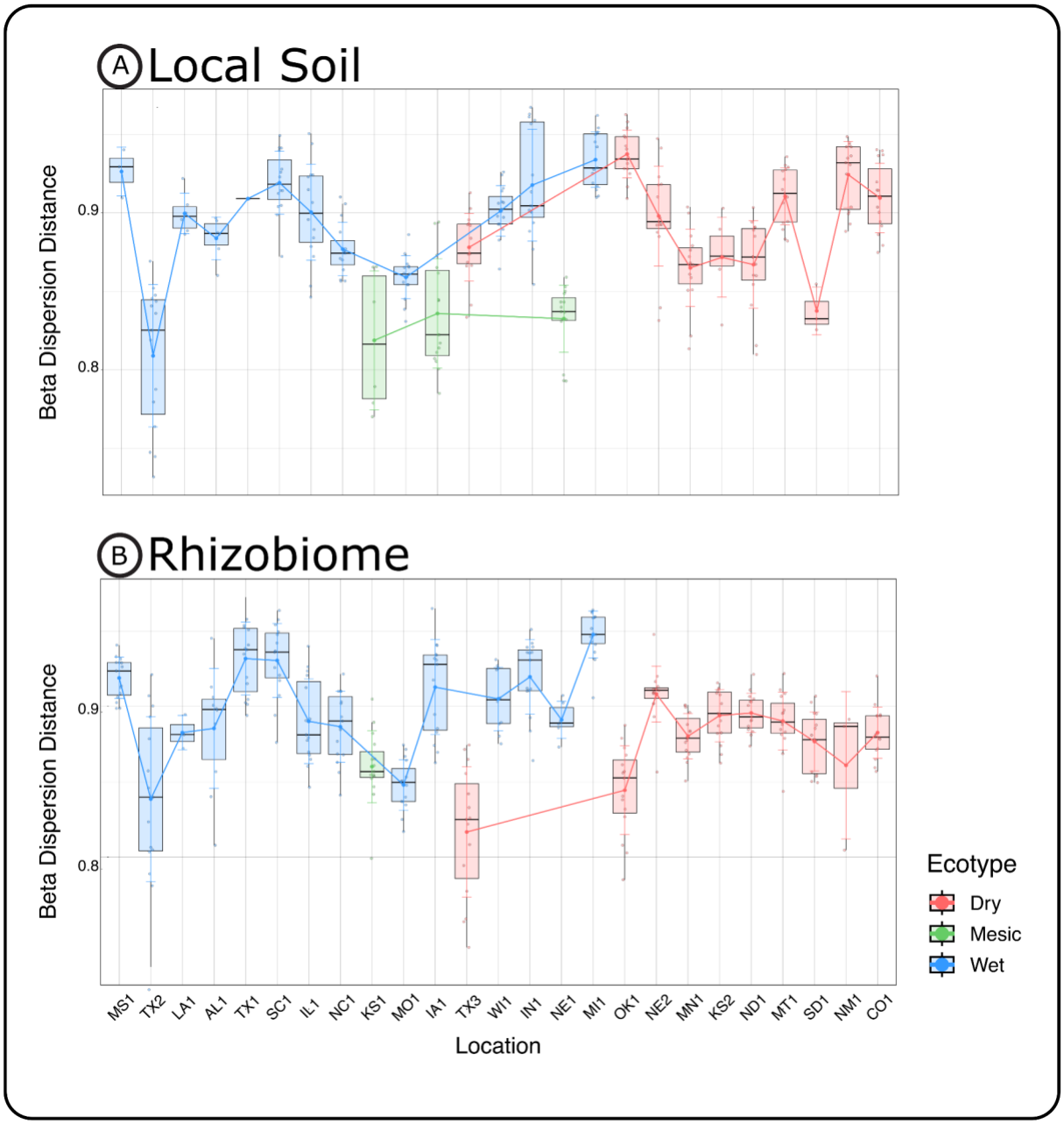
A Local Soil
Beta Dispersion Distance
0.9
0.8
B Rhizobiome
Beta Dispersion Distance
0.9
0.8
MS1
TX2
LA1
AL1
TX1
SC1
IL1
NC1
KS1
MO1
IA1
TX3
WI1
IN1
NE1
MI1
OK1
NE2
MN1
KS2
ND1
MT1
SD1
NM1
CO1
Location
Ecotype
Dry
Mesic
Wet

Figure 4

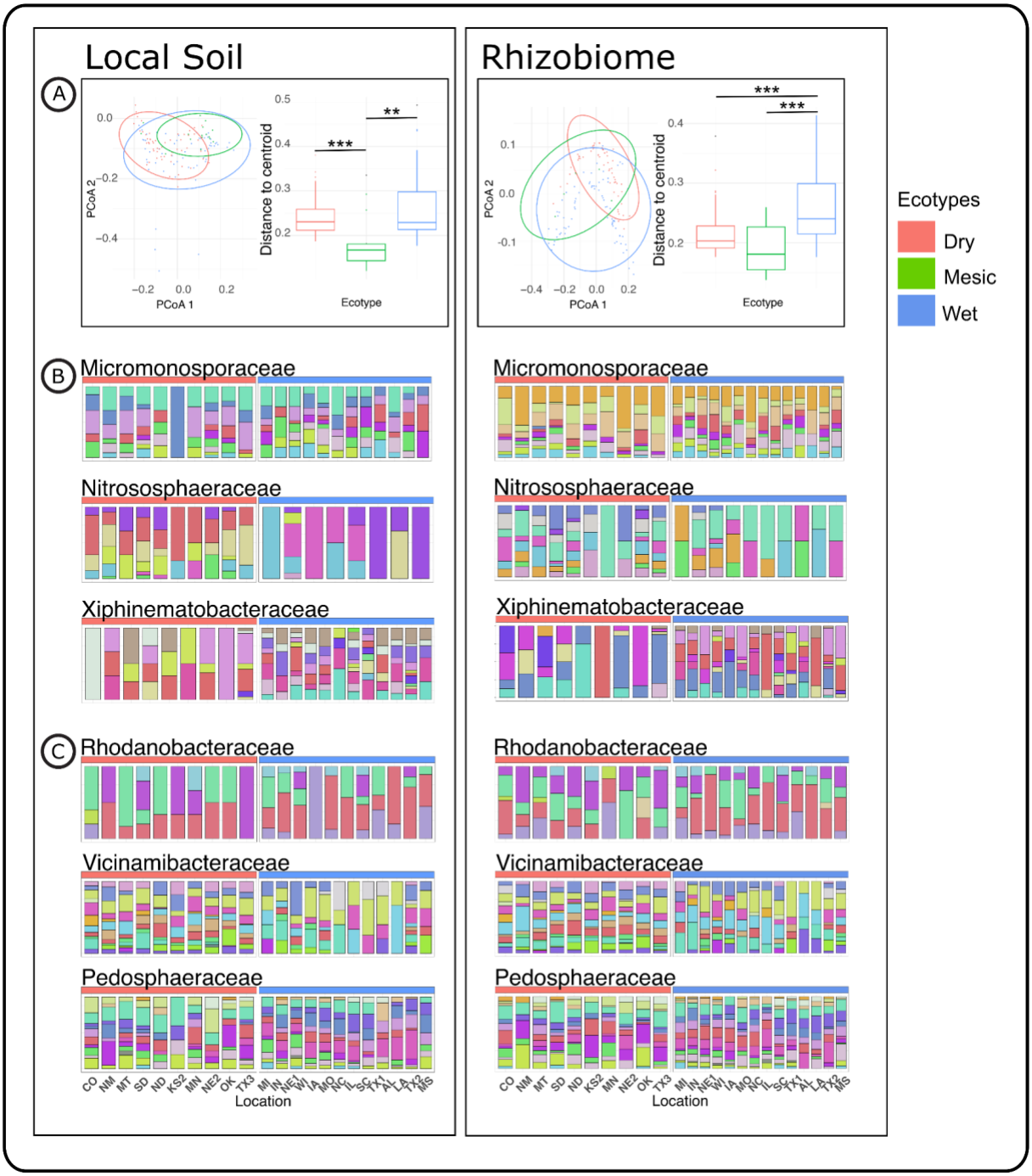
Local Soil
Rhizobiome
A
B
C
PCoA 1
PCoA 2
Distance to centroid
Ecotype
***
**
Micromonosporaceae
Nitrososphaeraceae
Xiphinematobacteraceae
Rhodanobacteraceae
Vicinamibacteraceae
Pedosphaeraceae
CO NM MT SD ND KS2 MN NE2 OK TX3 MI IN NE1 WI IA MO NC IL SC TX1 AL LA TX2 MS
Location
Ecotypes
Dry
Mesic
Wet

Figure 5

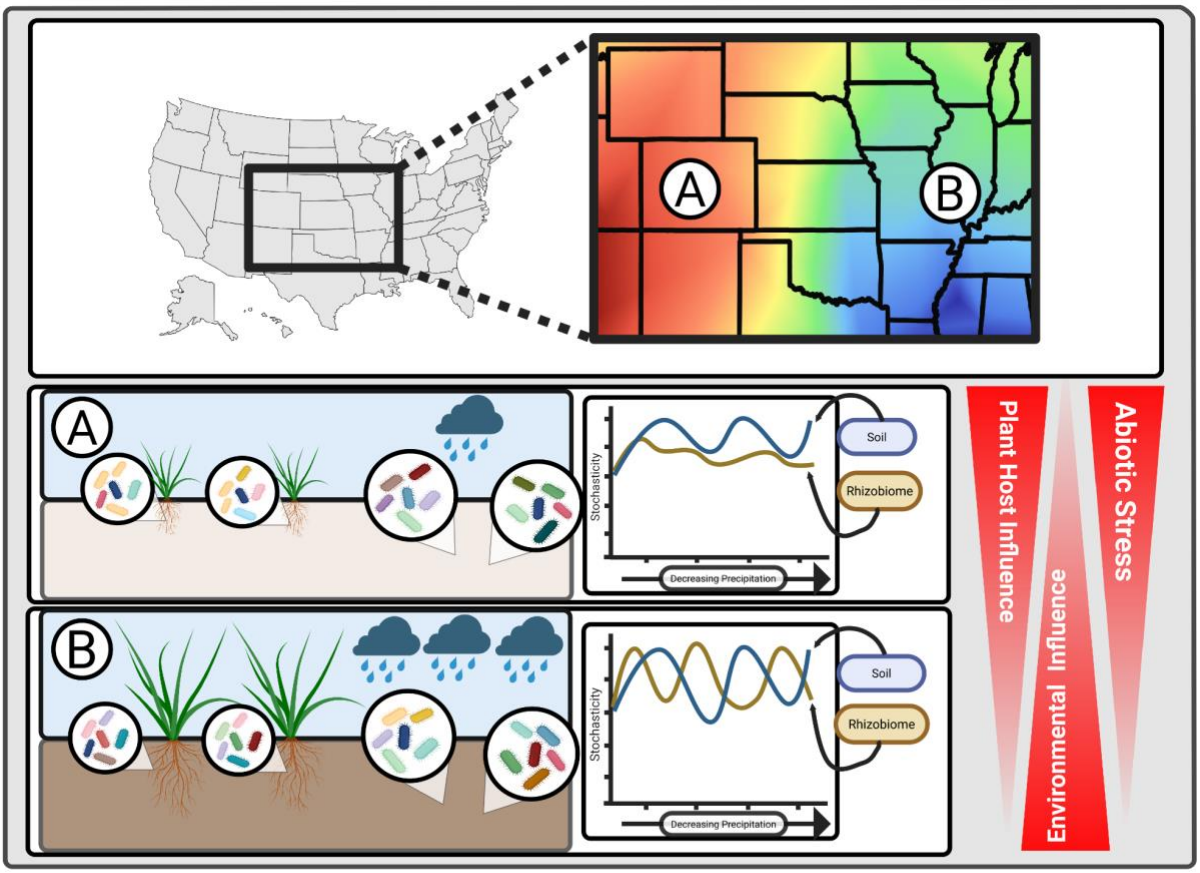
A
B
A
Stochasticity
Decreasing Precipitation
Soil
Rhizobiome
B
Stochasticity
Decreasing Precipitation
Soil
Rhizobiome
Plant Host Influence
Environmental Influence
Abiotic Stress

Figure 6